Supporting Information: Directional Design of Two-Dimensional SnSe Materials with High Thermopower Based on the Pareto Optimization

Shenshen Yan[1], Yi Wang[1], Zhibin Gao[1,2], Yang Long[1], and Jie Ren[1,3]*
[1]*Center for Phononics and Thermal Energy Science, China-EU Joint Lab on Nanophononics, Shanghai Key Laboratory of Special Artificial Microstructure Materials and Technology, School of Physics Science and Engineering, Tongji University, Shanghai 200092, China*
[2]*Department of Physics, National University of Singapore, Singapore 117551, Republic of Singapore and*
[3]*Shanghai Research Institute for Intelligent Autonomous Systems, Tongji University, Shanghai 200092, China*
(Dated: January 19, 2021)

I. CORRELATION BETWEEN BAND EFFECTIVE MASS AND DENSITY OF STATES EFFECTIVE MASS, AND SEEBECK COEFFICIENT FOR 3D AND 2D MATERIALS

Here, we show the different correlations between Seebeck coefficient and density of states (DOS) effective mass (m^*_{DOS}) for 3D and 2D materials. Meanwhile, we can also obtain the correlations between band effective mass (m^*_{band}) and density of states (DOS) effective mass (m^*_{DOS}) for 3D and 2D materials.

According to the Onsager reciprocal relations of the charge and heat currents [1]: $j_q = L^{(0)} \cdot \mathbf{E} + \frac{L^{(1)}}{qT} \cdot (-\nabla T)$, $j_Q = \frac{L^{(1)}}{q} \cdot \mathbf{E} + \frac{L^{(2)}}{q^2 T} \cdot (-\nabla T)$, where $L^{(\alpha)} = q^2 \int \sigma(E)(E - E_F)^\alpha (-\frac{\partial f(E)}{\partial E}) dE$, we can obtain the electronic conductivity and the Seebeck coefficient under the parabolic band model approximation: $\sigma_0 = L^{(0)}, S = \frac{1}{qT} \frac{L^{(1)}}{L^{(0)}}$, where the q, $\mathbf{E}$, E, T, E_F and $f(E)$ are the charge , electric field, energy, temperature, Fermi energy and Fermi-Dirac distribution function, respectively.

When only considering the electronic transport near the Fermi level, after performing a Sommerfeld expansion, we can obtain the Mott's relations [2]: $S = \frac{\pi^2 k_B^2 T}{3q} \frac{d[ln(\sigma(E))]}{dE}\Big|_{E=E_F}$. We can find that the DOS will make an important effect on the Seebeck coefficient.

The $\sigma(E)$ is the energy-dependent electronic conductivity, expressed as: $\sigma(E) = \tau(E) v^2(E) G(E)$, where the $\tau(E)$, $v(E)$ and $G(E)$ are the electronic relaxation time, group velocity of carriers and DOS of multiple degenerate bands. The DOS of multiple degenerate bands, $G(E)$ is determined by the DOS of single band: $G(E) = N_v g(E)$, where the N_v and $g(E)$ are band degeneracy and the DOS of single band respectively. If only considering the acoustic phonon scattering, we can get: $\tau(E) \propto E^{-1/2}$ [3]. According to the free electron approximation, the correlation between group velocity of carriers and energy is $v(E) \propto E^{1/2}$. Here we will give the DOS expression for 3D and 2D systems.

For 3D system, the DOS of single band model is: $g_{3D}(E) = \frac{1}{2\pi^2} (\frac{2m^*_{band}}{\hbar^2})^{3/2} E^{1/2}$ where $\hbar$ is reduced Planck constant. If considering the multiple degenerate bands model, the DOS of multiple degenerate bands model, $G_{3D}(E)$ is: $G_{3D}(E) = \frac{1}{2\pi^2} (\frac{2m^*_{DOS}}{\hbar^2})^{3/2} E^{1/2} = N_v g_{3D}(E)$. Then we can obtain that: $G_{3D}(E) = \frac{2}{2\pi^2} (\frac{2N_v^{2/3} m^*_{band}}{\hbar^2})^{3/2} E^{1/2}$. Therefore, we can find the correlation among the DOS effective mass, band degeneracy and single band effective mass for the 3D system[4, 5]: $m^*_{DOS} = N_v^{2/3} m^*_{band}$.

Similarly, for 2D system, the DOS of single band model is: $g_{2D}(E) = \frac{2}{(2\pi)^2} \frac{2\pi}{\hbar} m^*_{band}$. If considering the multiple degenerate bands model, the DOS of multiple degenerate bands model, $G_{2D}(E)$ is: $G_{2D}(E) = \frac{2}{(2\pi)^2} \frac{2\pi}{\hbar} m^*_{DOS} = N_v g_{2D}(E)$. Hence, we also can obtain that: $G_{2D}(E) = \frac{2}{(2\pi^2)} \frac{2\pi}{\hbar} N_v m^*_{band}$. We can also find the correlation among the DOS effective mass, band degeneracy and single band effective mass for the 2D system: $m^*_{DOS} = N_v m^*_{band}$. Then, we give the formulas of the Seebeck coefficient for 3D and 2D systems.

For 3D system, the energy-dependent electronic conductivity: $\sigma_{3D}(E) \propto E$, we could obtain the Seebeck coefficient:

*Xonics@tongji.edu.cn

$$
\begin{aligned}
S_{3D} &= \frac{\pi^2 k_B^2 T}{3q} \frac{d[ln(\sigma(E))]}{dE}\Big|_{E=E_F} \\
&= \frac{\pi^2 k_B^2 T}{3q} \frac{1}{E_F} \\
&= \frac{\pi^2 k_B^2 T}{3q} \frac{2m^*_{DOS,F}}{\hbar^2 k^2_{3D,F}} \\
&= \frac{2\pi^2 k_B^2 T}{3q\hbar^2} (\frac{1}{3\pi^2 n})^{2/3} m^*_{DOS,F}
\end{aligned}
\tag{1}
$$

where $m^*_{DOS,F} = \frac{\hbar^2 k_F^2}{2E_F}$ is the DOS effective mass at the Fermi energy level, k_F is the Fermi radius, the $k_{3D,F} = (3\pi^2 n)^{1/3}$ is the Fermi radius for 3D system, and n is carrier concentration.

Similarly, for 2D system, the energy-dependent electronic conductivity: $\sigma_{2D}(E) \propto E^{1/2}$, we could obtain the Seebeck coefficient:

$$
\begin{aligned}
S_{2D} &= \frac{\pi^2 k_B^2 T}{3q} \frac{d[ln(\sigma(E))]}{dE}\Big|_{E=E_F} \\
&= \frac{\pi^2 k_B^2 T}{3q} \frac{1}{2} \frac{1}{E_F} \\
&= \frac{\pi^2 k_B^2 T}{3q} \frac{1}{2} \frac{2m^*_{DOS,F}}{\hbar^2 k^2_{2D,F}} \\
&= \frac{\pi k_B^2 T}{6qn\hbar^2} m^*_{DOS,F}
\end{aligned}
\tag{2}
$$

where the $k_{2D,F} = (2\pi n)^{1/2}$ is the Fermi radius for 2D system.

II. THE THERMOPOWER ALONG X AND Y DIRECTIONS

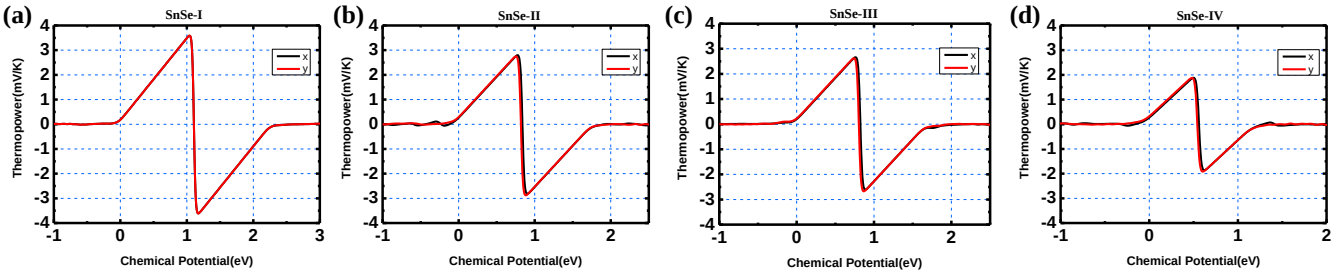

FIG. 1: There is thermopower of the four structures along x(black line) and y(red line) directions at 300K.

III. THE BILAYER STRUCTURES ON THE FIRST PARETO FRONT

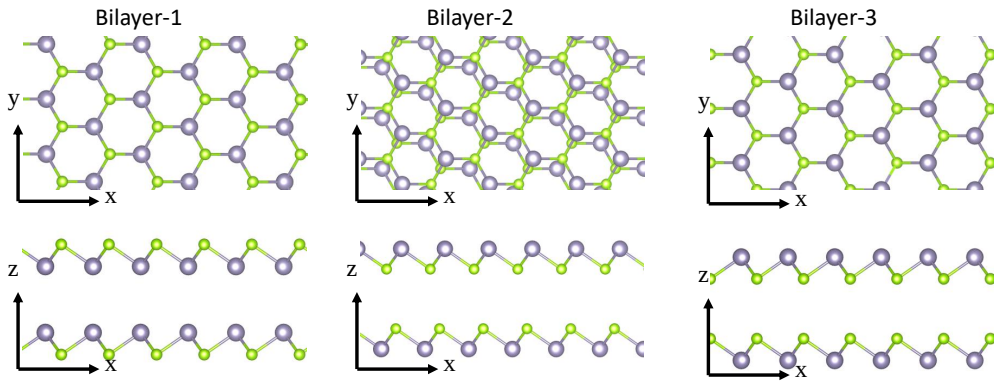

FIG. 2: There are three bilayer structures of 2D SnSe with the top and side views, which are blue hollow hexagonal symbols, as shown on the first Pareto Front.

TABLE I: Properties of three bilayer structures of 2D SnSe. There are space group, the values of lattice parameters a and b, free energy per atom and the values of thermopower, respectively.

Materials	Space group	a(Å)	b(Å)	E(eV/atom)	S(mV/K)
Bilayer-1	P-6m2	3.920	3.920	-4.081	2.829
Bilayer-2	P-1	3.913	3.915	-4.080	2.965
Bilayer-3	P-6m2	3.910	3.910	-4.079	2.968

IV. STRUCTURES ON THE SECOND PARETO FRONT AND THIRD PARETO FRONT

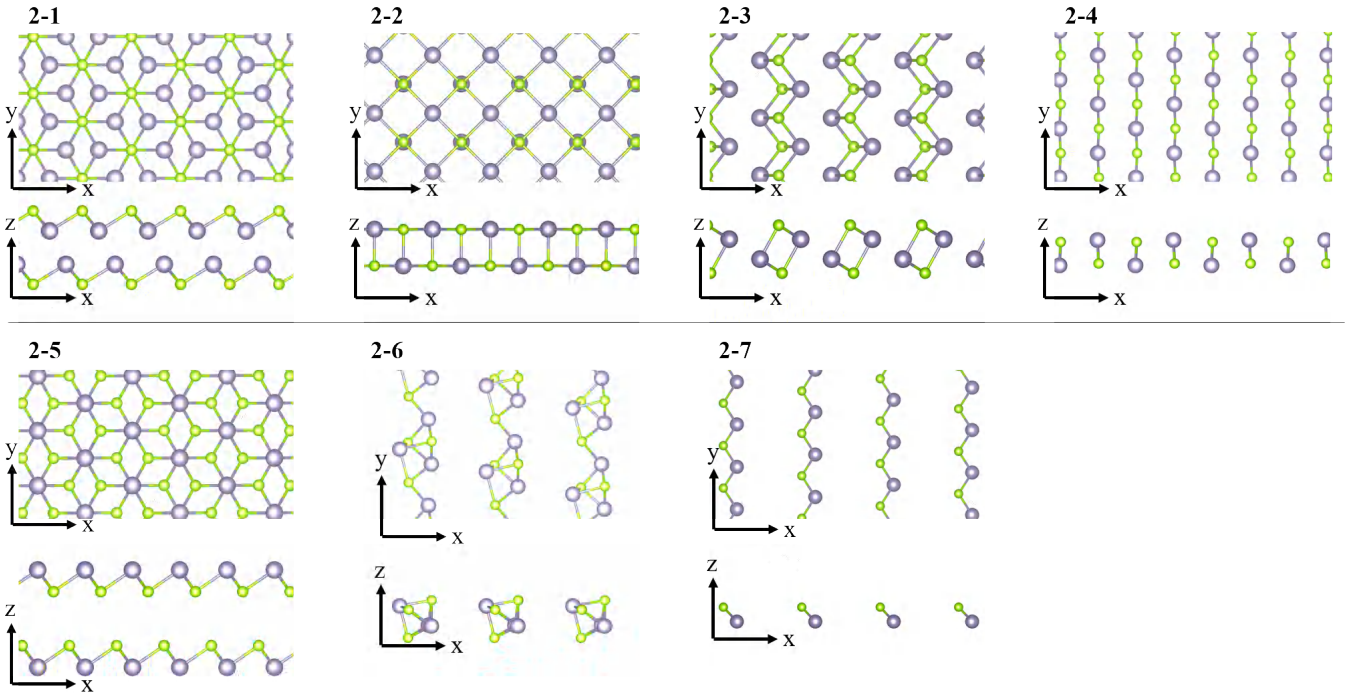

FIG. 3: Structures of 2D SnSe on the second Pareto Front are sorted by the free energy.

TABLE II: Properties of 2D SnSe structures on the second Pareto Front. There are space group, the values of lattice parameters a and b, free energy per atom and the values of thermopower, respectively.

Materials	Space group	a(Å)	b(Å)	E(eV/atom)	S(mV/K)
2-1	P-3m1	4.094	4.094	-4.137	0.887
2-2	Cmcm	4.320	4.320	-4.135	1.320
2-3	P-1	4.112	5.109	-4.105	1.555
2-4	Ama2	3.937	6.148	-4.103	2.719
2-5	C2/m	6.795	3.918	-4.080	2.906
2-6	P1	7.031	7.329	-3.990	2.914
2-7	P1	3.800	7.134	-3.794	2.971

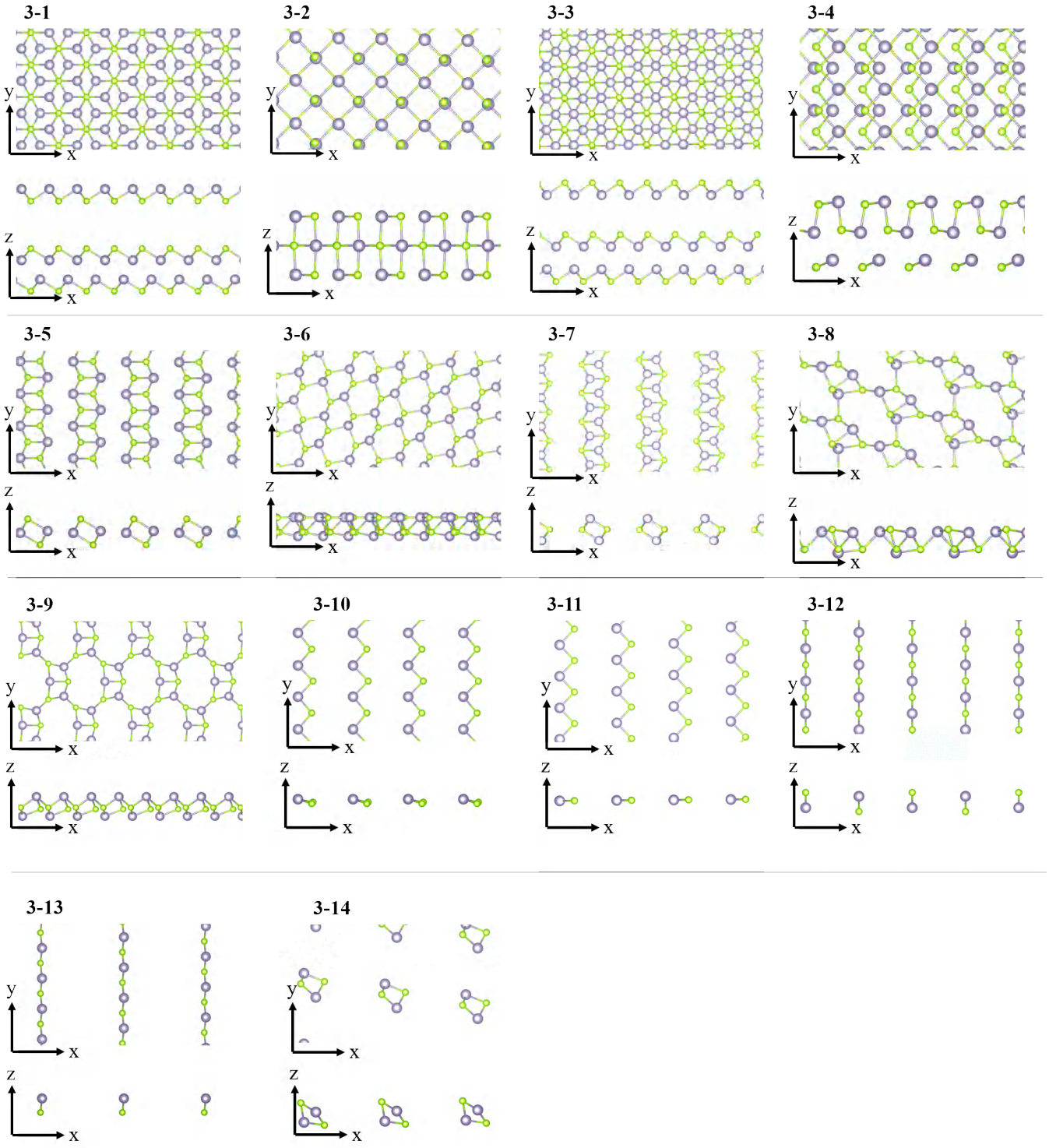

FIG. 4: Structures of 2D SnSe on the third Pareto Front are sorted by the free energy.

TABLE III: Properties of 2D SnSe structures on the third Pareto Front. There are space group, the values of lattice parameters a and b, free energy per atom and the values of thermopower, respectively.

Materials	Space group	a(Å)	b(Å)	E(eV/atom)	S(mV/K)
3-1	P3m1	4.039	4.039	-4.110	0.961
3-2	Cm	6.154	6.039	-4.107	1.003
3-3	Cm	6.825	3.989	-4.096	1.054
3-4	Pm	4.532	4.134	-4.077	1.359
3-5	P-1	3.911	6.410	-4.071	2.178
3-6	P1	6.516	6.501	-4.047	2.279
3-7	P-1	3.955	7.964	-4.034	2.720
3-8	P1	6.109	7.060	-4.027	2.762
3-9	P1	7.224	7.232	-3.986	2.775
3-10	Pm	6.594	7.615	-3.801	2.778
3-11	Amm2	3.793	13.768	-3.800	2.813
3-12	Pmmn	3.789	12.448	-3.797	2.894
3-13	P1	3.816	10.770	-3.787	2.963
3-14	P1	8.306	9.612	-3.738	2.970

[1] M. J. V. G. K. H. Madsen, J. Carrete, Comput. Phys. Commun. **231**, 140 (2018).
[2] G. Mahan and J. Sofo, Proc. Natl. Acad. Sci. U.S.A. **93**, 7436 (1996).
[3] V. I. K. A. S. G. D. L. Young, T. J. Coutts and W. P. Mulligan, J. Vac. Sci. Technol. **18**, 2978 (2000).
[4] T.-R. Wei, G. Tan, X. Zhang, C.-F. Wu, J.-F. Li, V. P. Dravid, G. J. Snyder, and M. G. Kanatzidis, J. Am. Chem. Soc. **138**, 8875 (2016).
[5] Z. M. Gibbs, F. Ricci, G. Li, Z. Hong, K. Persson, G. Ceder, G. Hautier, A. Jain, and G. J. Snyder, NPJ Comput. Mater. **3**, 1 (2017).